Supplementary Information

Fallen leaf-Sensitized Biosolar Oxygenation of Hydrocarbons

Minkyung Lee [a†], Jinha Jang [a†], Jeongeun Cha [b], Sang Hyun Lee [b], Frank Hollmann [c], Keehoon Won [d*], and Chan Beum Park [a*]

[a] Department of Materials Science and Engineering, Korea Advanced Institute of Science and Technology (KAIST), 335 Science Road, Daejeon 34141, Republic of Korea
[b] Department of Biological Engineering, Konkuk University, 120 Neungdong-ro, Gwangjin-gu, Seoul 05029, Republic of Korea
[c] Department of Biotechnology, Delft University of Technology, Van der Maasweg 9, 2629 HZ Delft, Netherlands.
[d] Department of Chemical and Biochemical Engineering, Dongguk University-Seoul, 30 Pildong-ro 1-gil, Jung-gu, Seoul 04620, Republic of Korea
*Corresponding authors. E-mail: keehoon@dongguk.edu; parkcb@kaist.ac.kr

Table of Contents

Fig S1. Photographs of kraft lignin and lignocellulosic wastes Photographs of kraft lignin and lignocellulosic waste powders (fallen Platanus leaves, waste wood, wastepaper, fallen pin oak leaves, fallen red maple leaves, softwood, and hardwood). Photo credit: Minkyung Lee, Korea Advanced Institute of Science and Technology.

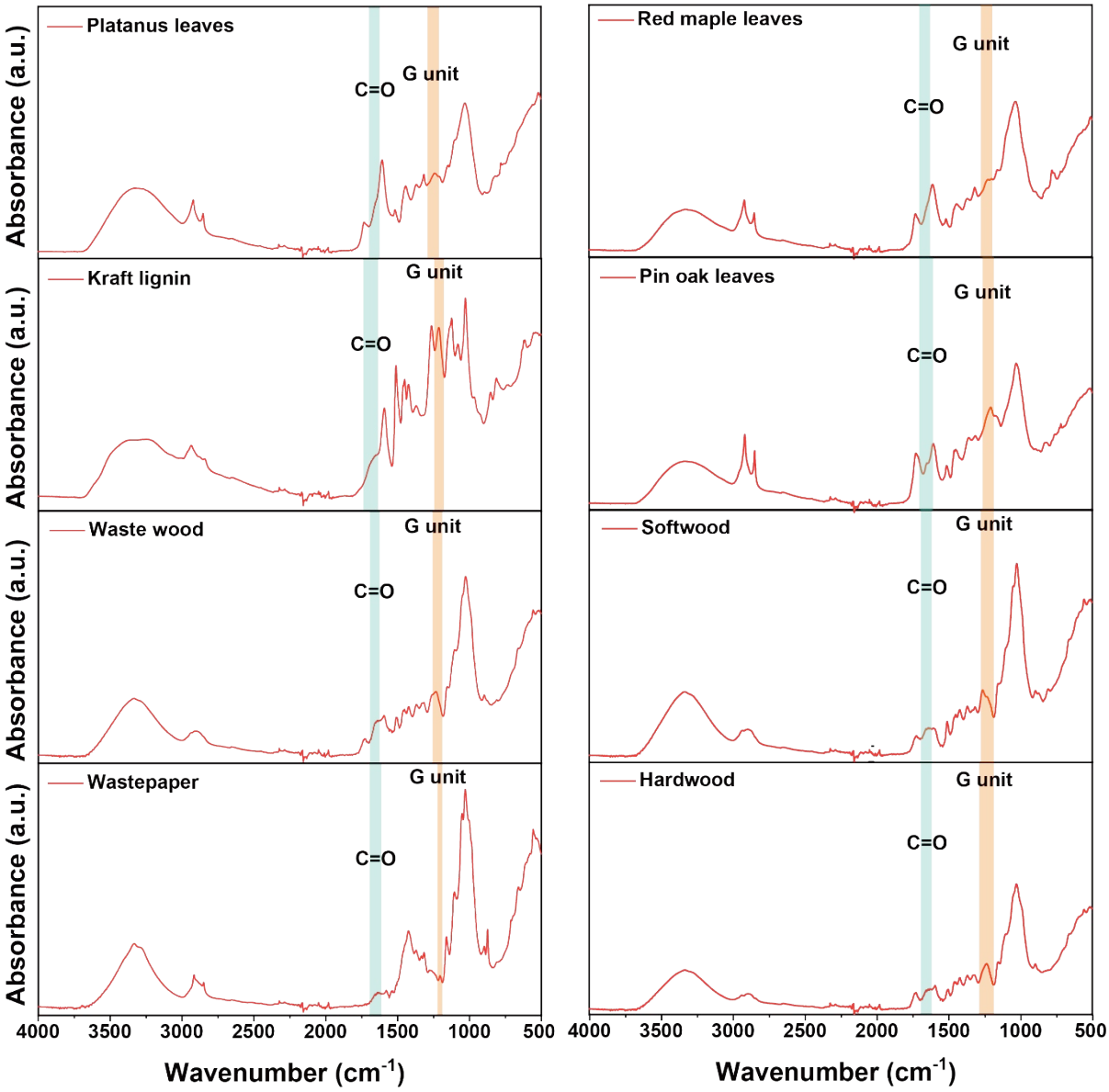

Fig S2. FT-IR spectra of lignocellulosic wastes FT-IR spectra of fallen Platanus leaves, kraft lignin, waste wood, wastepaper, fallen red maple leaves, fallen pin oak leaves, softwood, and hardwood in the region of 500–4000 cm^{-1}.

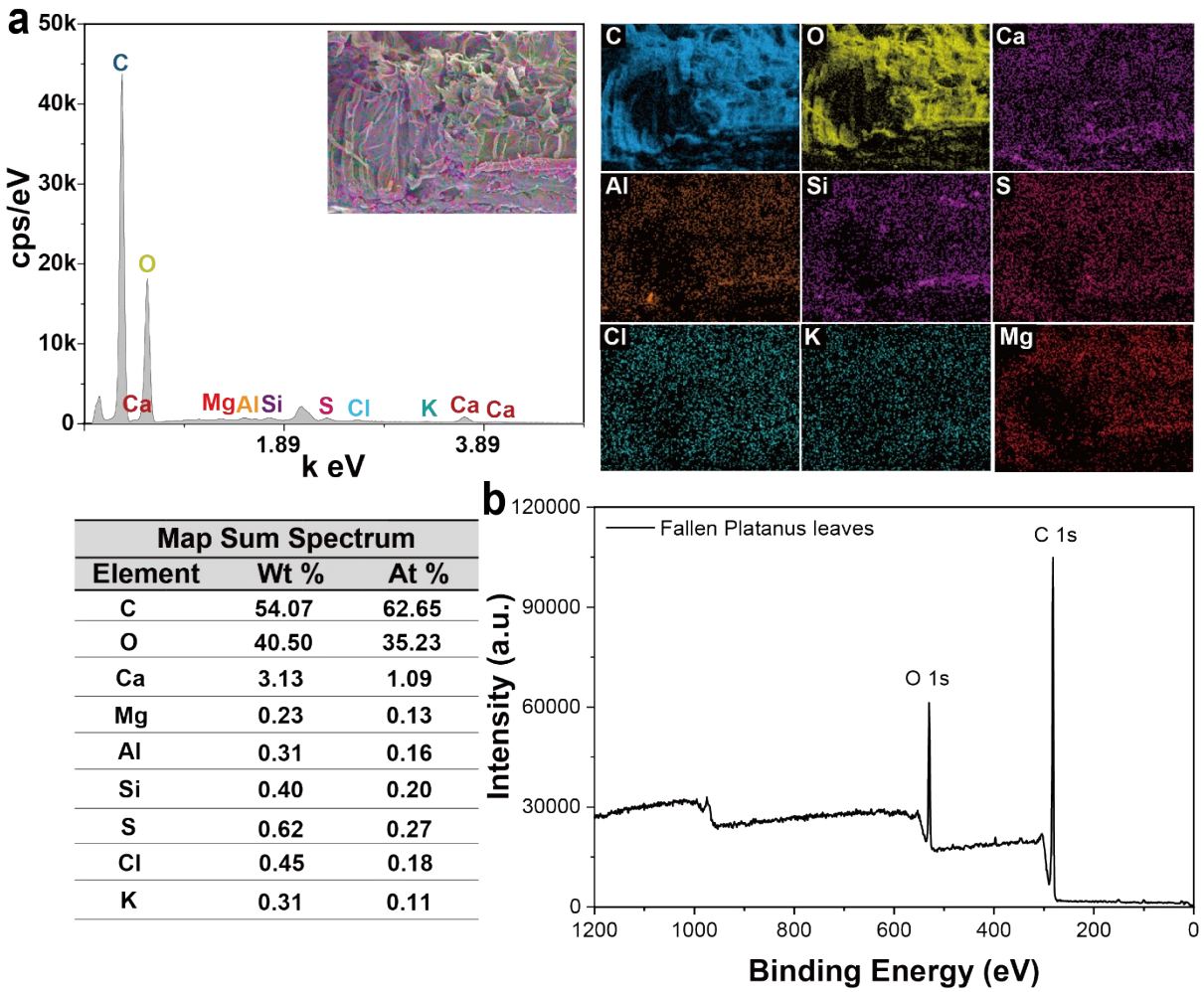

Map Sum Spectrum		
Element	Wt %	At %
C	54.07	62.65
O	40.50	35.23
Ca	3.13	1.09
Mg	0.23	0.13
Al	0.31	0.16
Si	0.40	0.20
S	0.62	0.27
Cl	0.45	0.18
K	0.31	0.11

Fig S3. Characterization of the fallen Platanus leaves a, SEM-EDS spectrum, images, and elemental compositional table b, XPS spectrum

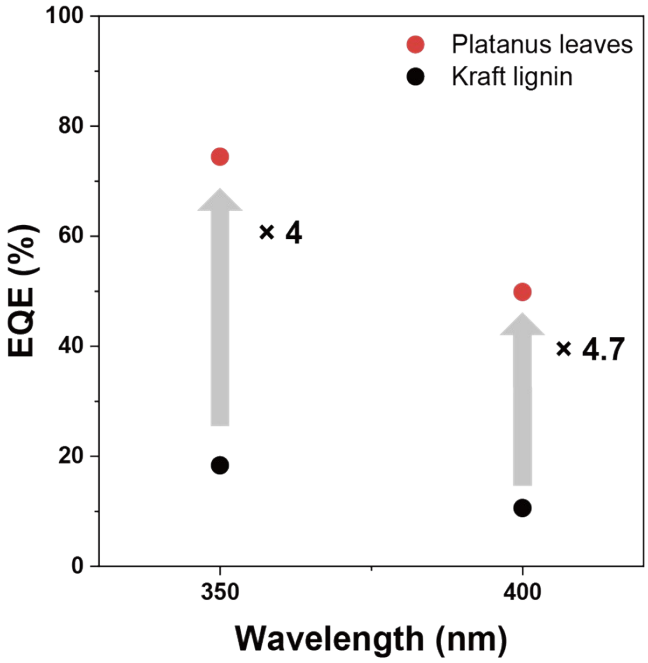

Fig S4. External quantum efficiency (EQE) of the fallen Platanus leaves and kraft lignin

External quantum efficiency (EQE) of H_2O_2 production under monochromator-selected illumination (350 and 400 nm; illuminated area 4.24 cm^2; irradiance 10 mW cm^{-2}; 30 min) for 1 mg mL^{-1} of the fallen Platanus leaves and kraft lignin.

$$(6)\ External\ Quantum\ Efficiency\ (EQE) = 2\frac{nH2O2}{nphoton} X\ 100\ (\%)$$

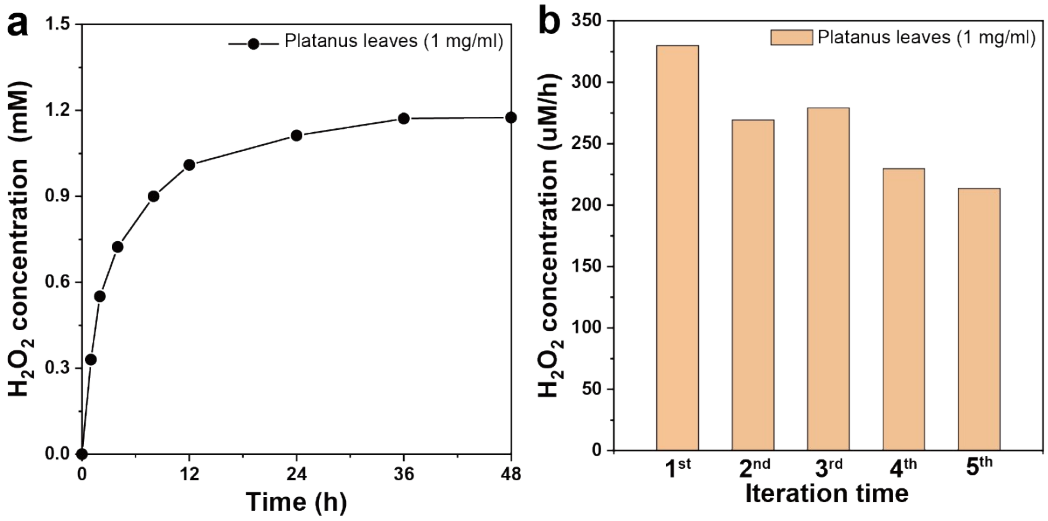

Fig S5. Long-term stability and reusability test of the fallen Platanus leaves (a) Time profiles of H_2O_2 production by the fallen Platanus leaves (1 mg/mL) in a KPi buffer (100 mM, pH=7) under O_2/light for 48 h (b) Reusability test of fallen Platanus leaves (1 mg/mL) for H_2O_2 production in 100 mM KPi buffer (pH 7) under O_2 and visible light irradiation for 1 h. After each cycle, the leaves were washed with water before reusing.

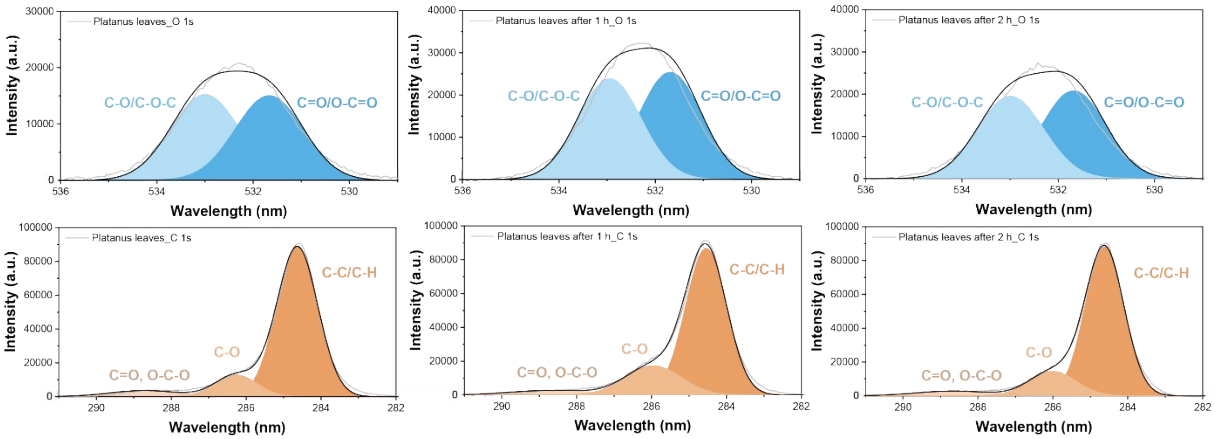

Fig S6. XPS C 1s and O 1s spectra of Platanus leaves before (0 h) and after 1 h and 2 h of photochemical reaction

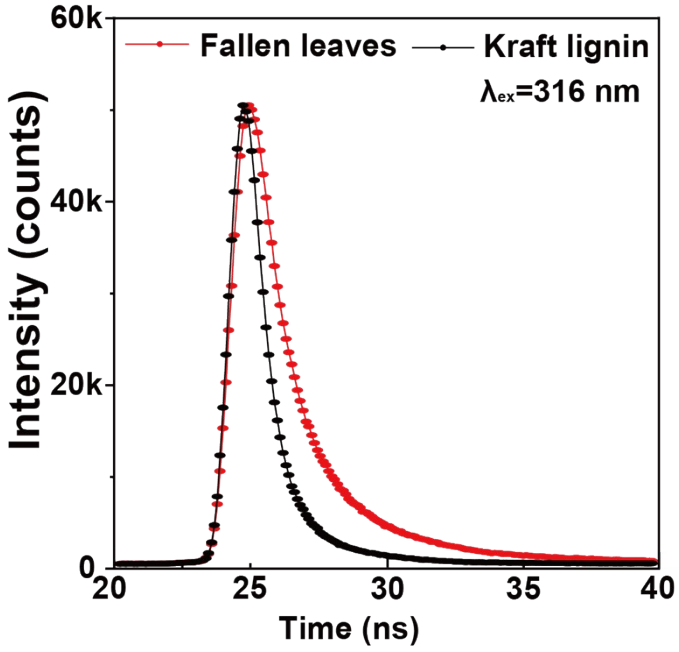

Fig S7. Time-resolved spectroscopic analysis of kraft lignin and the fallen Platanus leaves. Time-resolved fluorescence decay profiles of the fallen Platanus leaves (red) and kraft lignin (black) at excitation wavelength = 316 nm in a KPi (100 mM, pH=7). Powder concentration: 0.1 mg/mL. These decay profiles were fitted to a quadruple-exponential function: the fallen Platanus leaves: τ_1 = 1.4 ns, τ_2 = 3.4 ns, and τ_3 = 9.6 ns, τ_4 = 0.6 ns with average fluorescence lifetime = 1.5 ns; kraft lignin: τ_1 = 0.5 ns, τ_2 = 1.7 ns, and τ_3 = 5.4 ns, τ_4 = 0.4 ns with average fluorescence lifetime = 0.5 ns.

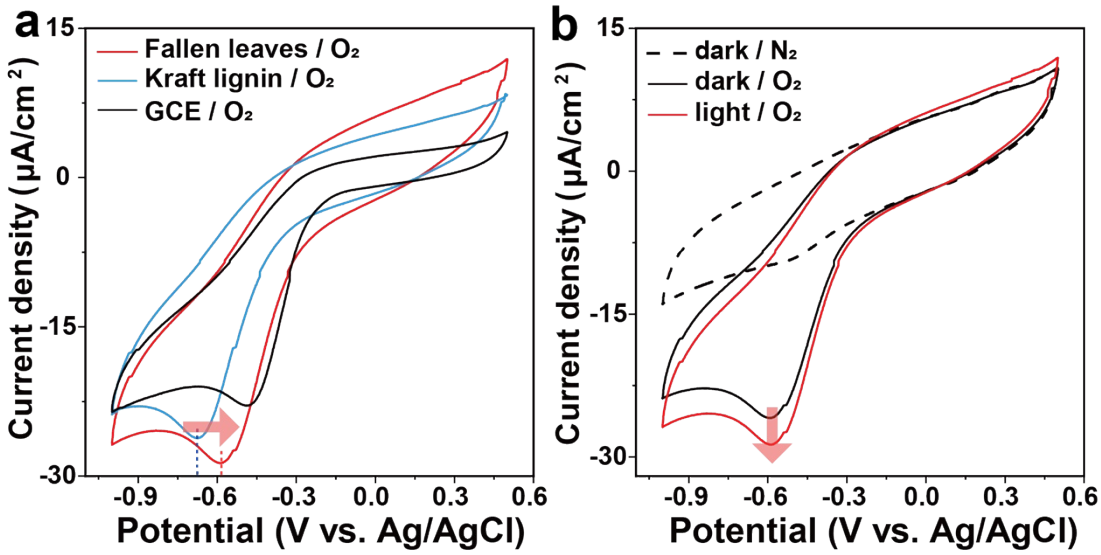

Fig S8. Cyclic voltammetry of the fallen Platanus leaves and kraft lignin (a) Cyclic voltammograms of glassy carbon electrode (black), kraft lignin (blue), the fallen Platanus leaves (red) in an O_2-saturated KPi buffer (100 mM, pH=7) under light (260 nm < λ < 900 nm, I = 100 mW/cm^2). **(b)** Cyclic voltammograms of the fallen Platanus leaves under dark/N_2 (black, dotted), dark/O_2 (black, solid), and light/O_2 (red) in a KPi buffer (100 mM, pH=7). Scan rate: 50 mV/s; the number of cycles: 3.

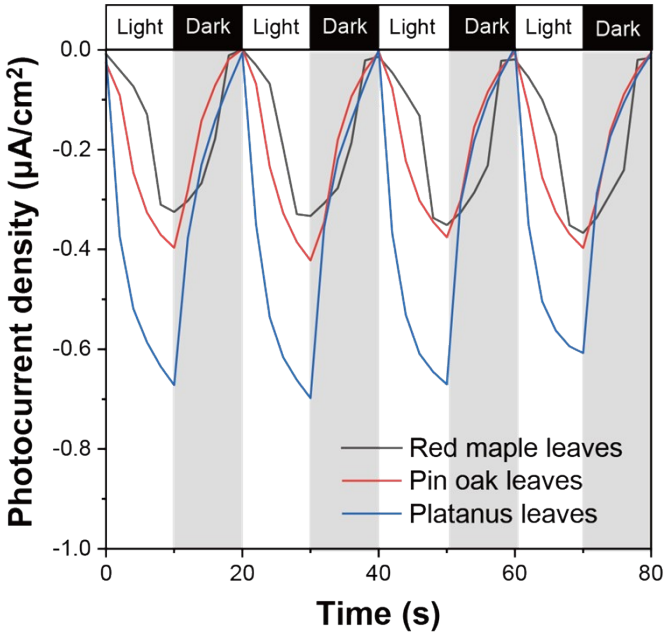

Fig S9. Transient photocurrent responses of defoliated leaves. Chopped CA at –0.6 V vs Ag/AgCl under intermittent light irradiation of Platanus leaves (blue), red maple leaves (black), and pin oak leaves (red).

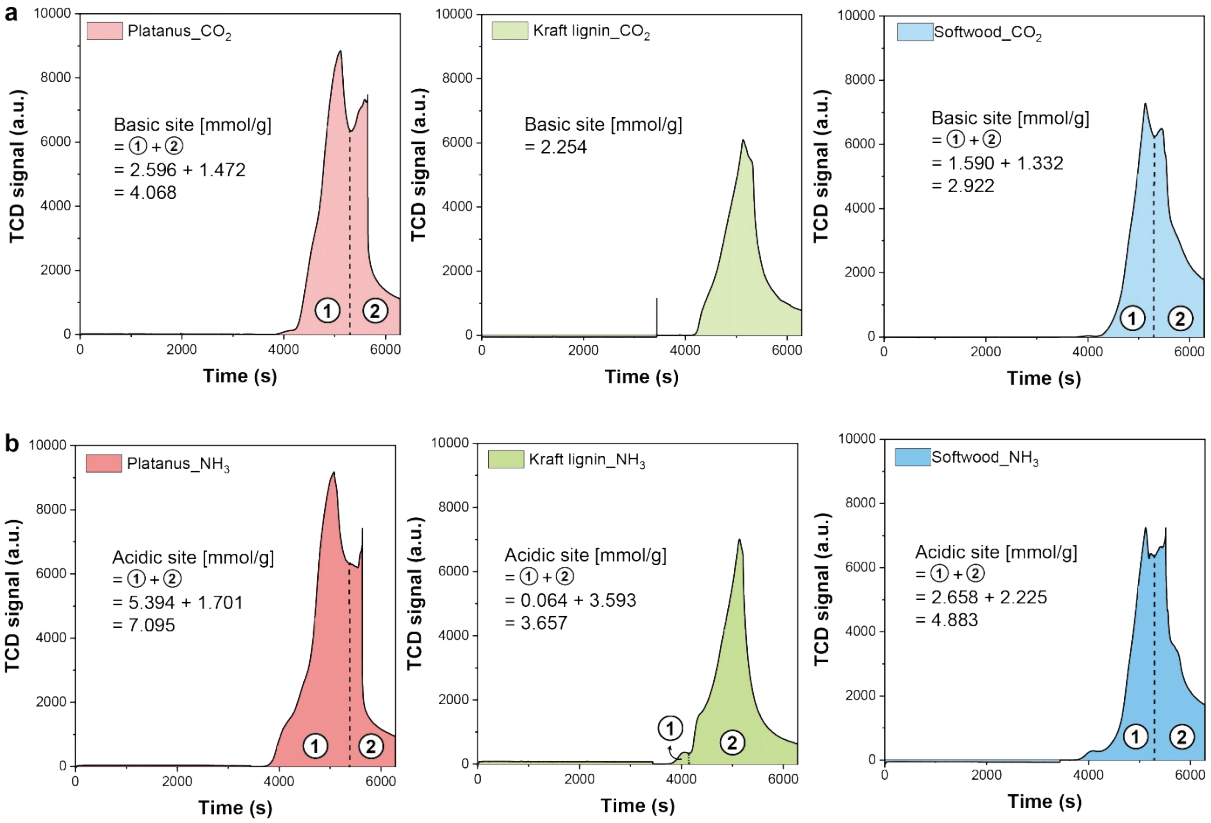

Fig S10. Temperature-programmed desorption (TPD) analysis. (a) CO_2-TPD (b) NH_3-TPD of Platanus leaves, kraft lignin, and softwood.

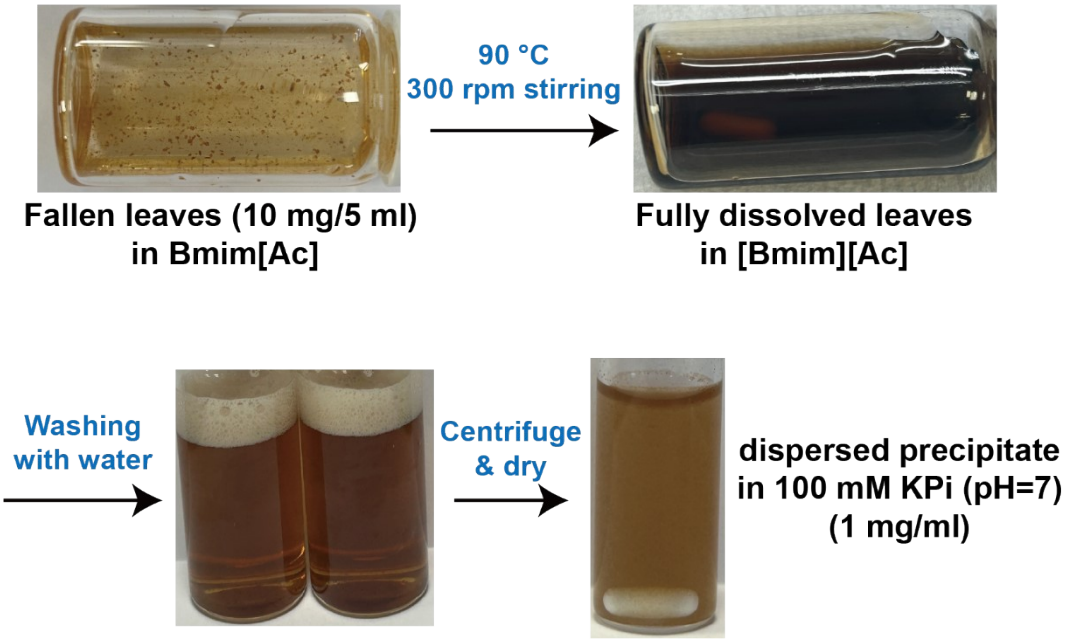

Fig S11. Dissolution processes of the fallen Platanus leaves followed by reassembly process Photographs of the dissolution and reassembly processes in ionic liquid ([Bmim][Ac]) of the fallen Platanus leaves.

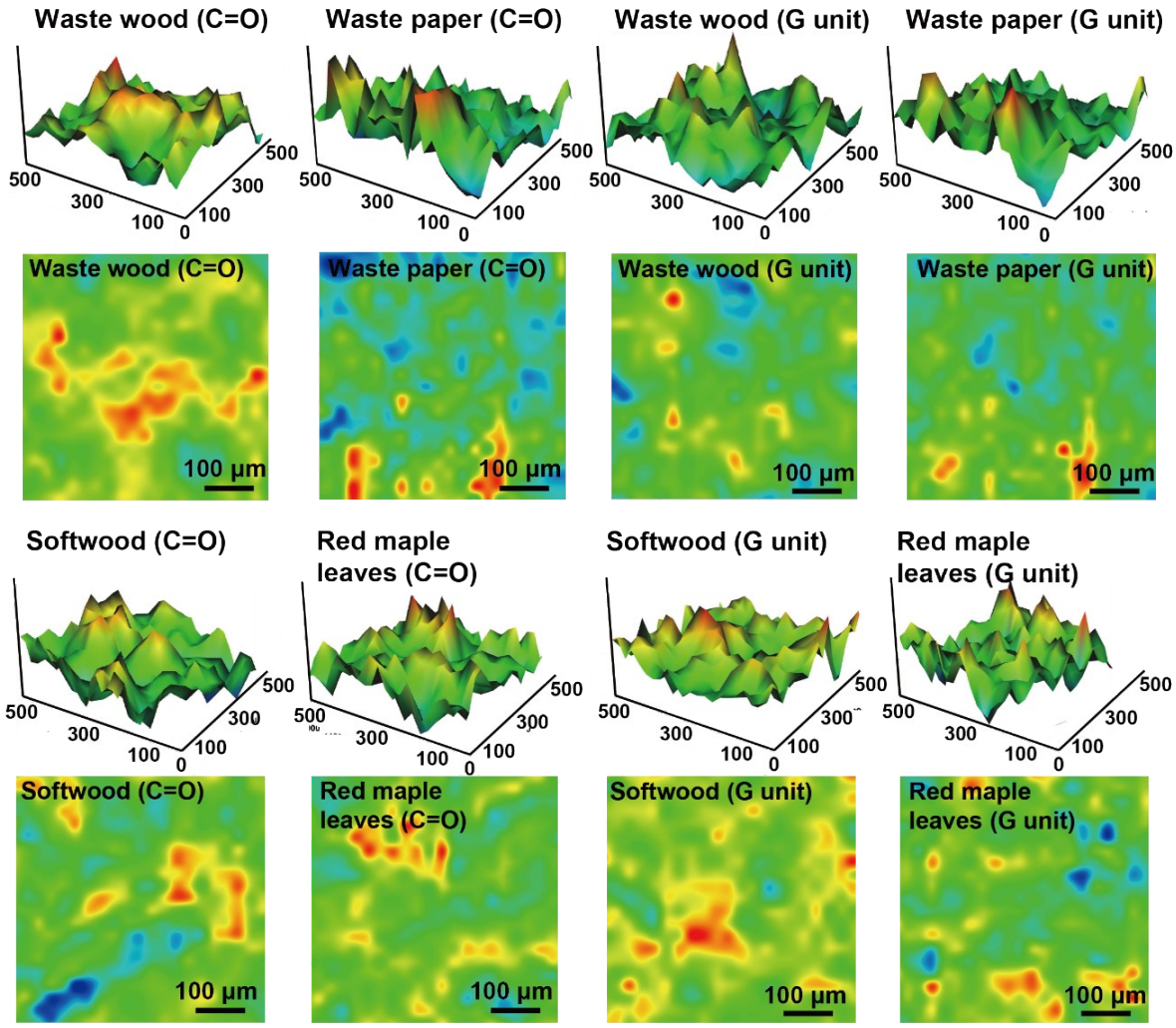

Fig S12. FTIR spectroscopic images and corresponding intensity images FT-IR 3D and 2D images for the C=O (1600–1700 cm^{-1}) group and G unit (1100–1250 cm^{-1}) of waste wood, wastepaper, softwood, and fallen red maple leaves.

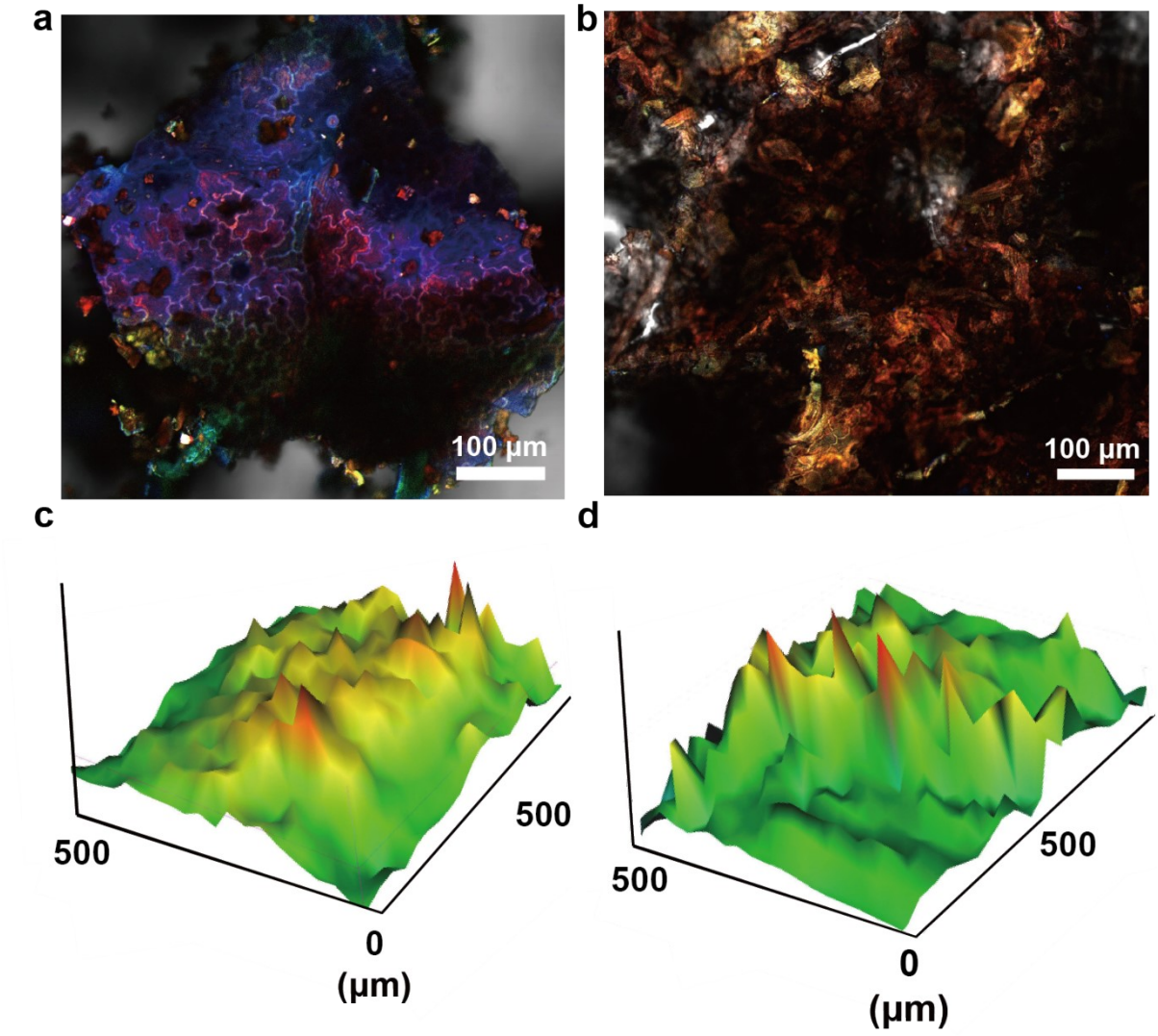

Fig S13. Characterization of the fallen Platanus leaves before and after reassembly process. Confocal image of the fallen Platanus leaves (a) before and (b) after reassembly process, FTIR spectroscopic images after reassembly process at (c) 1150 cm^{-1} and (d) 1650 cm^{-1}.

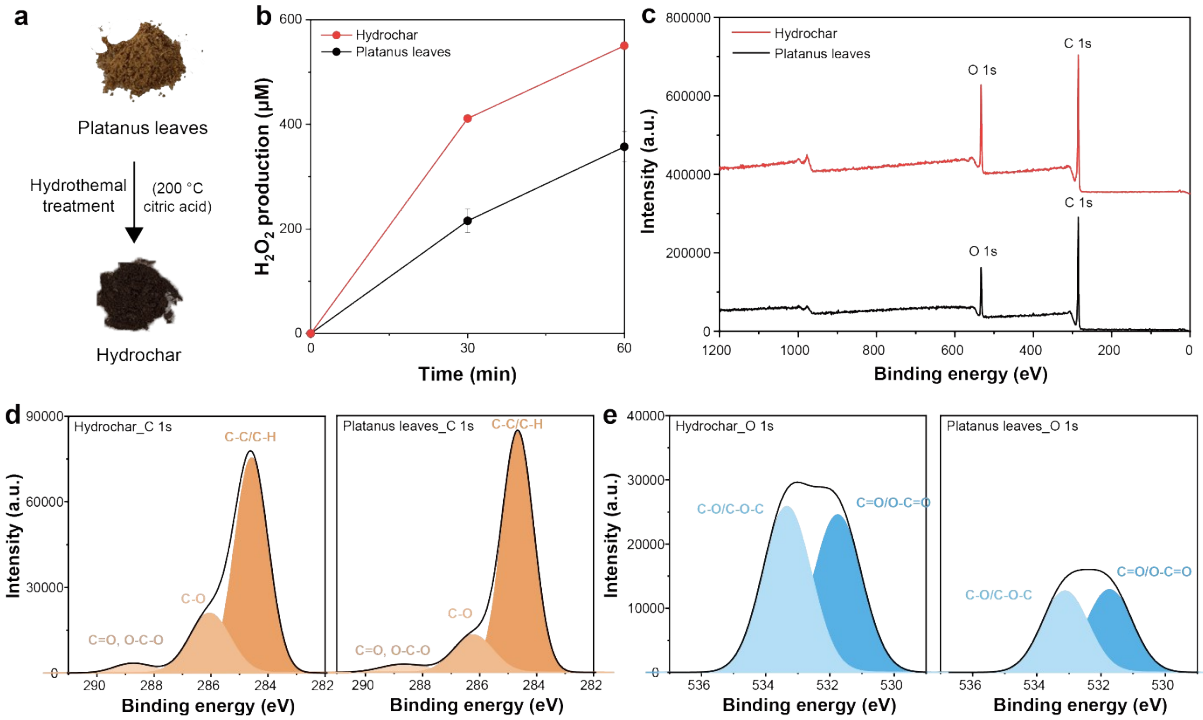

Fig S14. Comparison of untreated Platanus leaves and hydrochar. (a) Photographs/SEM images of the Platanus leaves and the hydrochar prepared by hydrothermal treatment with citric acid. (b) Time profiles of photocatalytic H_2O_2 production for Platanus leaves and the hydrochar under O_2-purged illumination. (c) Survey scan XPS spectra, (d) C 1s spectra, and (e) O 1s spectra of Platanus leaves and hydrochar.

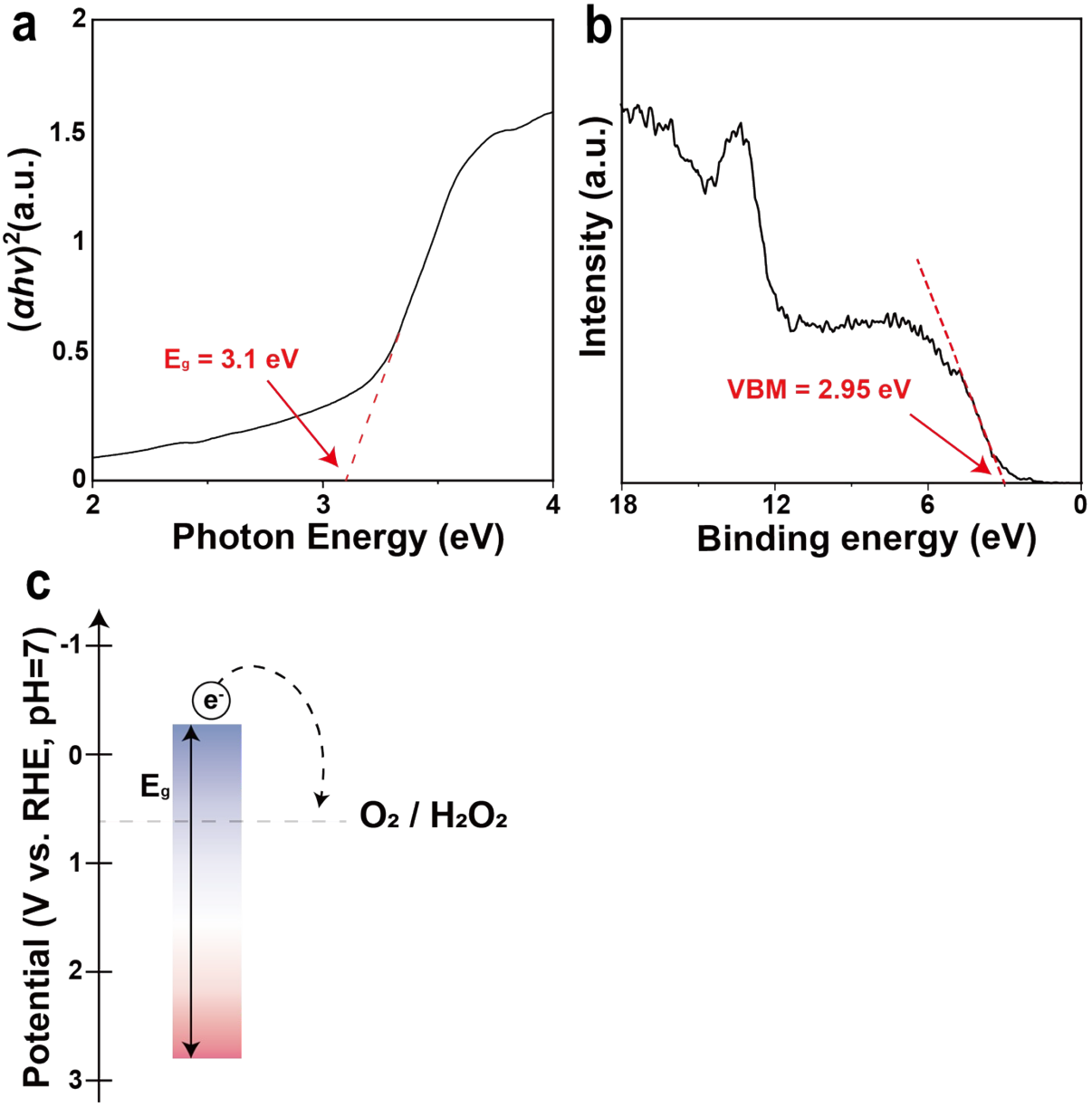

Fig S15. Photophysical properties of the fallen Platanus leaves (a) Tauc plot to estimate its optical bandgap of the fallen leaves (0.01 mg/mL). (b) XPS valence band spectra. (c) Energy diagram for the fallen Platanus leaves. E_g: optical bandgap.

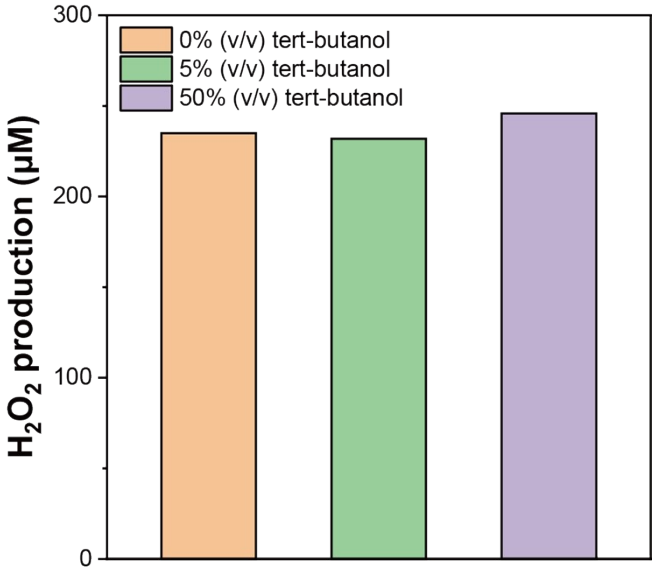

Fig S16. Effect of hydroxyl radical scavenger on H_2O_2 generation of Platanus leaves H_2O_2 production by *Platanus* leaves was evaluated under O_2-purged conditions in 100 mM KPi buffer (pH=7) containing 0%, 5%, or 50% (v/v) tert-butanol as a hydroxyl radical scavenger to analyze the effect of hydroxyl radical scavenging on photocatalytic two-electron.

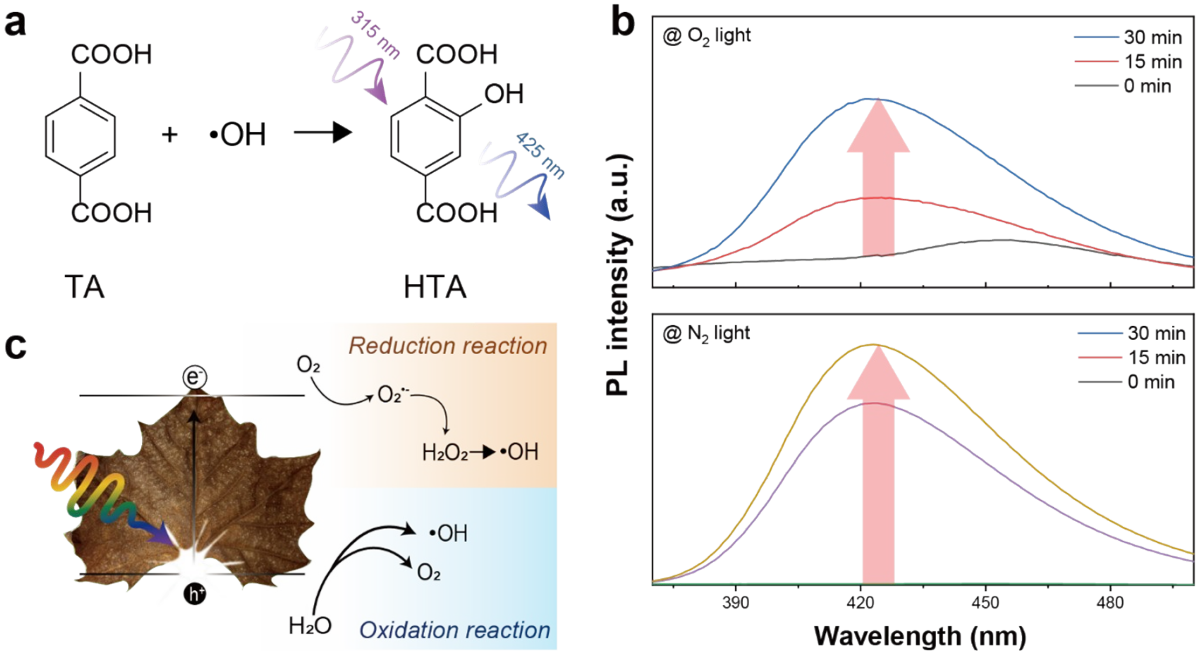

Fig S17. Identification of hydroxyl radical formation and reaction pathways in the Platanus-driven photocatalytic system. (a) Reaction scheme of terephthalic acid (TA) oxidation by hydroxyl radicals. (b) TA assay showing hydroxyl radical generation during photocatalytic reaction by Platanus leaves under O_2 light condition (upper) and N_2 light condition (lower). (c) Proposed reaction pathways for oxygen reduction and water oxidation under illumination.

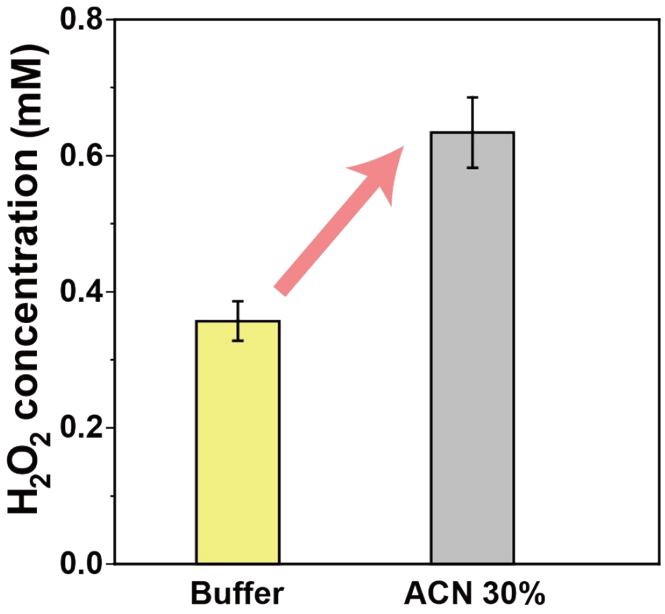

Fig S18. Effect of cosolvent on the rate of H_2O_2 production The fallen Platanus leaf-driven H_2O_2 generation in different solutions. Reaction conditions: photocatalyst (1 mg/mL) in a KPi buffer (100 mM, pH=7), 30% (w/w) acetonitrile (ACN) in the KPi buffer under light (260 nm $< \lambda <$ 900 nm, I = 100 mW/cm^2) with O_2 purging at room temperature after 1 h.

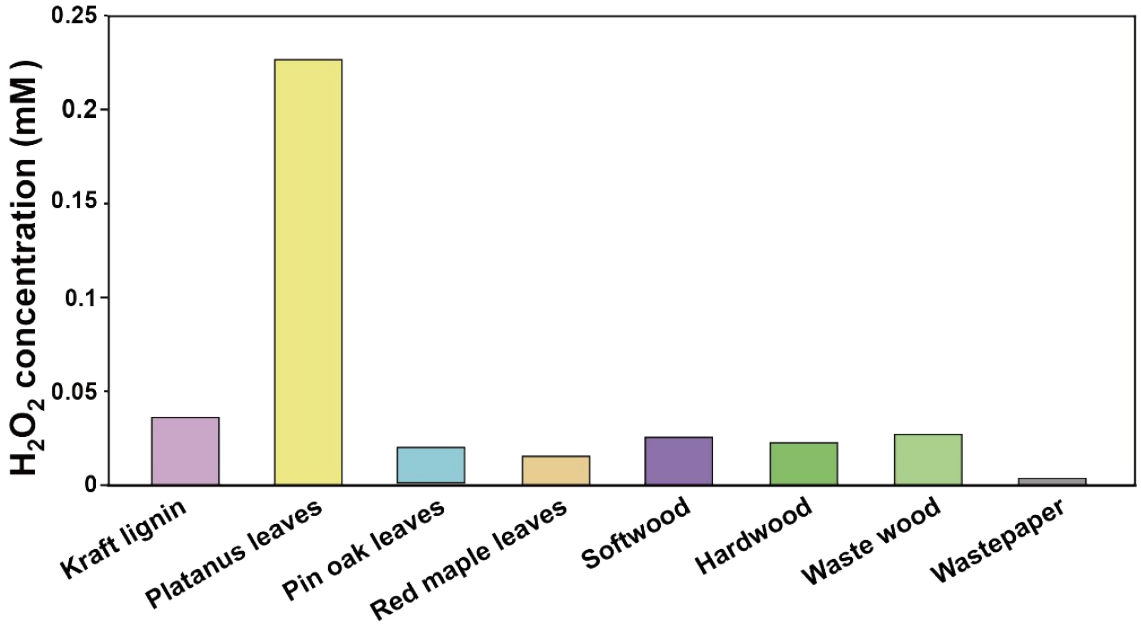

Fig S19. H_2O_2 production from kraft lignin and lignocellulosic wastes (5 mg/ml) under visible light.

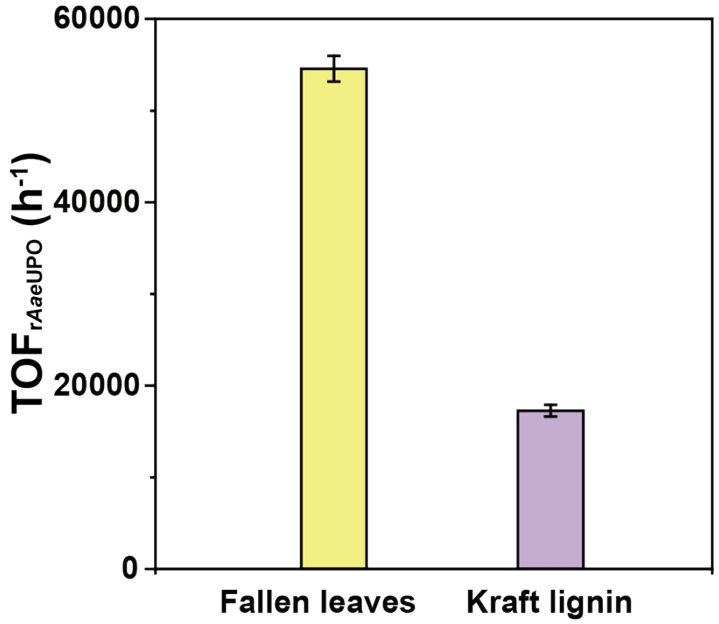

Fig S20. Kinetics of photocatalyst/*Aae*UPO hybrid's photoenzymatic hydroxylation reaction Photoenzymatic reaction by the fallen Platanus leaves and kraft lignin. Reaction conditions: photocatalyst (5 mg/mL), *Aae*UPO (10 nM), and ethylbenzene (10 mM) in a KPi buffer (100 mM, pH=7) with O_2 purging under visible light (400 nm < λ < 900 nm, I = 100 mW/cm^2) at room temperature. The TOF_{AaeUPO} was measured after the reaction for 30 min.

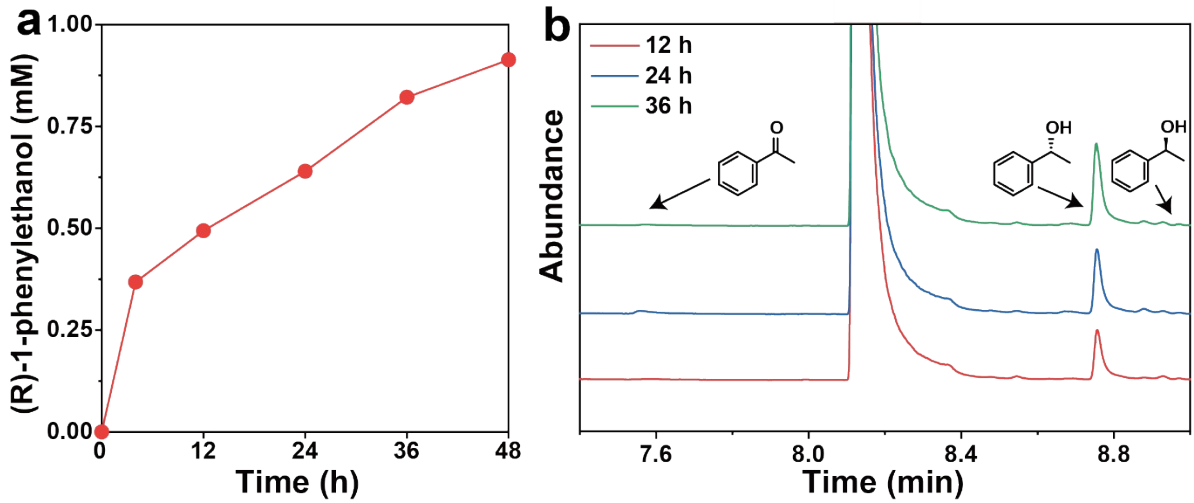

Fig S21. Photoenzymatic systems for ethylbenzene hydroxylation (a) Time profiles of (*R*)-1-phenylethanol from ethylbenzene hydroxylation driven by the fallen Platanus leaf/*Aae*UPO hybrid catalyst. Reaction conditions: 5 mg/mL, 10 nM *Aae*UPO, and 10 mM ethylbenzene in a KPi buffer (100 mM, pH=7) under visible light (400 nm < λ < 900 nm, I = 100 mW/cm^2) at room temperature upon O_2 purging (b) The gas chromatogram during the photoenzymatic reaction of ethylbenzene

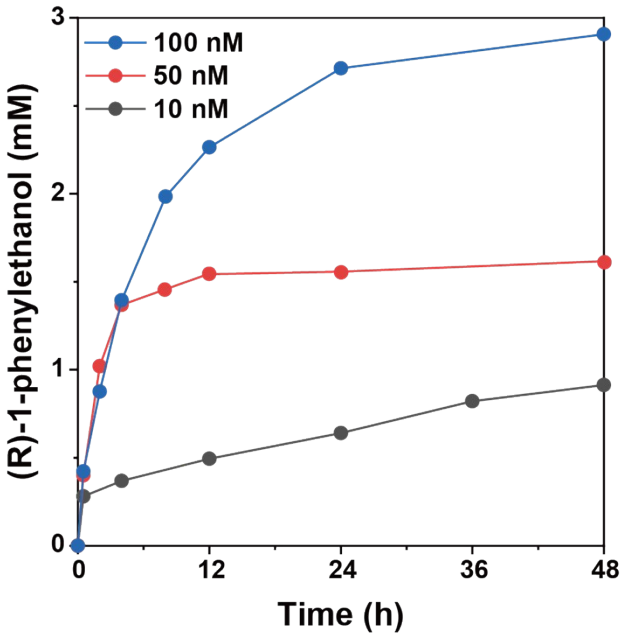

Fig S22. Effect of enzyme loading on the concentration of (R)-1-phenylethanol production

Time profiles of (*R*)-1-phenylethanol from ethylbenzene hydroxylation driven by the fallen Platanus leaf/*Aae*UPO hybrid catalyst. Reaction conditions: 5 mg/ml, 10, 50, 100 nM *Aae*UPO, and 10 mM ethylbenzene in a KPi buffer (100 mM, pH=7) under visible light (400 nm < λ < 900 nm, I = 100 mW/cm^2) at room temperature upon O_2 purging.

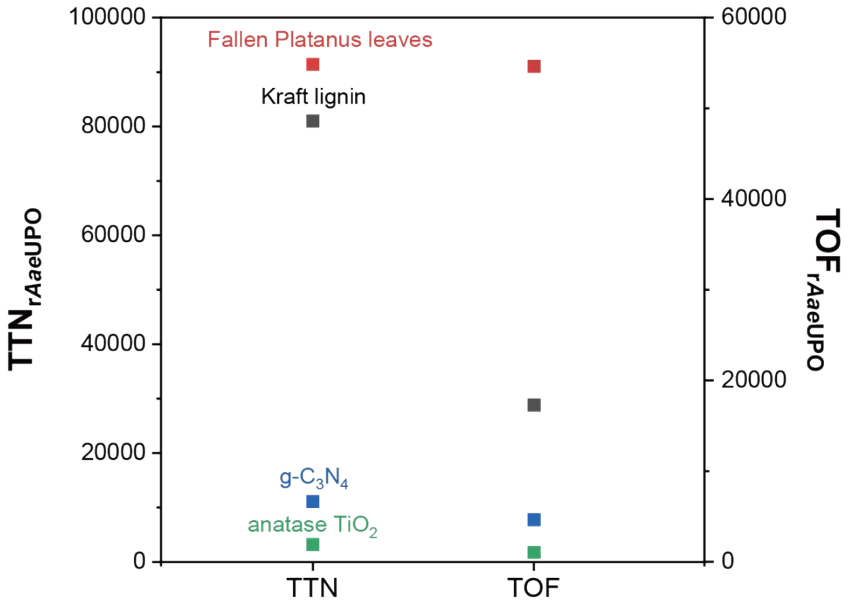

Fig S23. Comparison of TTN_{AaeUPO} and TOF_{AaeUPO} values for photoenzymatic ethylbenzene hydroxylation

Table S1. Gas chromatography conditions for quantification of analytes

Substrate	Temperature profile	Retention time (min)
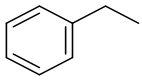 Ethylbenzene	60 °C for 5 min 20 °C/min to 130 °C, hold for 6 min 40 °C/min to 180 °C, hold for 2 min 20 °C/min to 200 °C, hold for 3 min	(R)-1-phenylethanol: 8.9 (S)-1-phenylethanol: 9.1 Acetophenone: 7.6 1-octanol: 8.2
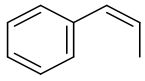 *cis*-β-methylstyrene	60 °C for 5 min 10 °C/min to 130 °C, hold for 5 min 40 °C/min to 180 °C, hold for 2 min 20 °C/min to 200 °C, hold for 3 min	*cis*-β-methylstyrene: 6.3 (1*R*,2*S*)- *cis*-β-methylstyrene oxide: 9.1 (1*S*,2*R*)- *cis*-β-methylstyrene oxide 9.3 1-octanol: 9.7
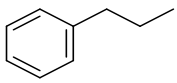 Propylbenzene	60 °C for 5 min 20 °C/min to 130 °C, hold 6 min 40 °C/min to 180 °C, hold for 2 min 20 °C/min to 200 °C, hold for 3 min	Propylbenzene: 4.8 (R)-1-phenyl-1-propanol: 9.6 (S)-1-phenyl-1-propanol: 9.7 1-octanol:8.1
 Cyclohexane	60 °C for 5 min 20 °C/min to 130 °C, hold 6 min 40 °C/min to 180 °C, hold for 2 min 20 °C/min to 200 °C, hold for 3 min	Cyclohexanone:5.3 Cyclohexanol: 7.1 1-octanol: 8.2

Table S2. Compositional analysis of lignocellulosic wastes

Sample	Glucan	Hemicellulose	Acid-soluble lignin	Acid-insoluble lignin	Ash	Extractives
Platanus leaves	11.8 ± 0.3	4.8 ± 0.4	0.5 ± 0.0	46.1 ± 0.7	0.9 ± 0.1	12.8
Red maple leaves	9.1 ± 0.4	7.5 ± 0.3	0.5 ± 0.0	19.1 ± 0.8	3.1 ± 0.4	38.3
Pin oak leaves	10.2 ± 0.2	8.9 ± 0.2	2.2 ± 0.0	25.7 ± 0.4	0.0 ± 0.0	30.5
Waste wood	36.4 ± 0.5	12.2 ± 0.1	0.8 ± 0.0	31.5 ± 0.7	0.0 ± 0.0	5.9
Softwood	35.2 ± 0.4	17.4 ± 0.3	0.3 ± 0.0	27.7 ± 0.1	0.0 ± 0.0	8.6
Hardwood	35.2 ± 0.7	16.4 ± 0.3	0.8 ± 0.1	25.4 ± 0.7	0.0 ± 0.0	7.4
Wastepaper	56.6 ± 0.5	14.8 ± 0.2	0.5 ± 0.0	8.3 ± 0.6	0.6 ± 0.1	5.1